JABFM
eISSN 2280-8000

J Appl Biomater Funct Mater 2017; 15 (Suppl 1): S52-S61
DOI: 10.5301/jabfm.5000358

ORIGINAL RESEARCH ARTICLE

Open Access

Chemical modification of bagasse-based mesoporous carbons for chromium(III) ion adsorption

Haiwen Ma, Kunquan Li, Qiangfei Chai

College of Engineering, Nanjing Agricultural University, Nanjing - China

ABSTRACT

Aims: Modified bagasse-based mesoporous carbons were prepared for the efficient chromium(III) ion adsorption and removal from aqueous solutions.

Methods: Mesoporous carbons were prepared from bagasse with H3PO4 activation and subsequently oxidized with nitric acid and modified with ethylenediamine.

Results: The results showed that the modified carbon was rich in mesopores, oxygen and nitrogen-containing groups, and the Cr(III) adsorption capacity was greatly improved after modification, which was found to be higher than both pristine and oxidized carbons. The Cr(III) adsorption capacity on modified carbon was significantly influenced by the solution pH, and the optimum pH was 6 with the maximum Cr(III) adsorption capacity up to 24.61mg/g, which was almost 3 times higher than that for pristine carbon. Thermodynamic results manifested the adsorption was spontaneous and endothermic. Kinetic rates fitted the pseudo-second-order model very well. XPS study indicated the amino group was a key factor of the high efficient adsorption.

Keywords: Amino group, Bagasse, Chemical modification, Chromium(III) ion, Mesoporous carbon

Introduction

Chromium is one of the most common heavy metals in the industry. Chromium pollution in our environment mainly derives from ore processing, metal surface treatment, leather tanning, printing and dyeing (1). The chromium ion canenter the human body through the food chain, putting people in danger of brain damage, pulmonary edema and renal damage (2). At present, the methods of dealing with chromium wastewater are various in China and abroad, mainly including chemical precipitation, biosorption, ion exchange and adsorption (3). But most of these methods have certain deficiencies, such as the production of chromium sludge, low removal efficiency and high cost (4). However, compared with other methods, the adsorption has various advantages including easy operation, no secondary pollution, low costs and high efficiency (5). It has been proven that as a common adsorbent the activated carbon is widely used for its developed pore structure and high specific surface area(S_{BEC}), which contributes to its high adsorption capacity, better economic effect, and sustainability (6).

Accepted: April 11, 2017
Published online: May 29, 2017

Corresponding author:
Kunquan Li
College of Engineering
Nanjing Agricultural University
210031 Nanjing, China
kqlee@njau.edu.cn

Researches have shown that the adsorption of heavy metal on activated carbon includes physical and chemical adsorption (7), the former is mainly controlled by its S_{BEC} and pore structure. The pore structure of carbon includes three types: micropore (<2 nm), mesopore (2-50 nm) and macropore (>50 nm) (8). These three pore structures play diverse roles in the adsorption. For instance, macropore primarily acts as a channel from which the adsorbate molecule gets into the carbon (9); mesopore can be used as a channel for the entrance of metal ion to micropore, as well as the macromolecular, which is inaccessible to micropore; micropore is generally known as the absorbed pore as it contributes to the developed S_{BEC} and pore volume of activated carbons (10). However, the chemical adsorption or electrostatic adsorption mainly depends on the surface chemical property of activated carbon, which influences the interaction between the carbon and polar solution as well as the nonpolar solution (11). Oxygen and nitrogen-containing groups can greatly affect the adsorption capacity on activated carbon by influencing the carbon's surface reaction, catalytic properties, zeta potential and surface charge (12). Therefore, according to the characteristics of the adsorption, it is worthwhile to study the pore structure and surface chemistry of activated carbon for its significant improvement in adsorption capacity.

As sugarcane is one major crop in China, with a cultivation area surpassing 2.0 million hectares, as much as 450,000 tons (dry weight) of bagasse are produced annually. Since bagasse with high carbon content and is easy to obtain, a better way for the exploitation of this cheap and abundant agricultural by-product is to turn it into activated

carbon. This research prepared bagasse-based mesoporous carbons from bagasse and introduced polyamine groups by nitric acid oxidation and amide reaction for the enhanced Cr(III) adsorption. Surface properties of the pristine, oxidized and modified carbons were performed by fourier transformed infrared spectroscopy (FTIR), nitrogen adsorption/desorption and x-ray photoelectron spectroscopy (XPS). The kinetic rates of adsorbents were modeled by using the pseudo-first-order and pseudo-second-order. The adsorption performance of the modified carbon for the removal of Cr(III) was tested and compared with pristine and oxidized carbons, as well as other adsorbents reported in earlier studies. Besides, the effect of modification condition, initial concentration, temperature and solution pH on the Cr(III) adsorption onto modified carbon were examined, and the adsorption mechanism of Cr(III) on modified carbon was also discussed.

Materials and methods

Reagent and instrument

The following reagents were used: high purity nitrogen (99.999%), phosphoric acid (H_3PO_4), nitric acid (HNO_3), ethylenediamine (EDA), chromic nitrate ($Cr(NO_3)_3$, anhydrous salt), dicyclohexylcarbodiimide (DCC), and these chemical reagents were of analytical grade. Main instruments included ASAP-2020 Micromeritics instrument (American Micromeritics Co., Ltd), TENSOR27 FTIR infrared spectrometer (Germany Bruke Co., Ltd), 250XI ESCALAB x-ray photoelectron spectrometer (American Thermo Electron Co., Ltd), high-temperature tubular furnace (BLMT-1200°C, Nanjing Yudian automation technology Co., Ltd).

Samples preparation, modification and characterization

Preparation of sample

The raw material bagasse was smashed and sifted through mesh number 50 (about 0.3 mm) and then soaked for 24 h with H_3PO_4solution with an impregnation ratio of 1:1.5 (weight of bagasse/weight of phosphoric acid), which has been proven as the optimum parameters for preparing mesoporous carbon by our previous study (13). Then the soaked precursors were dried in a high temperature furnace at 105°C for 8 h. Afterwards, the carbonization of acid-impregnated bagasse was carried out under high purity nitrogen flow of 40 mL/min by raising the temperature at a rate of 5°C/min until activation temperature reached 500°C and kept at this temperature for 90 minutes. Then the activated materials were cooled to ambient temperature under the flow of gaseous nitrogen. To obtain the final adsorbents, HCl solution (0.1 mol/L) was used to remove impurities in pyrolytic materials under 60°C water bath with strong stirring for 3 h. Afterwards, the resulting materials were rinsed with deionized water in a soxhlet extractor until the washing water pH ranged from 6.0 to 7.0, and then dried at 80°C for 24 h to obtain the pristine carbon AC. The yield of prepared AC at this condition was up to 35.8%.

Modification of sample

The oxidation process was carried out by adding 150 mL HNO_3(17.5%) to 5 g of dried AC in the Erlenmeyer flask. The mixed materials were placed in the magnetic stirrer with strong stirring for 6 h at 60°C to obtain the oxidized carbon marked as AC-HNO_3. At last, the modified process was implemented by adding 75 mL EDA solution to 5 g of AC-HNO_3, after stirring well 5 g of DCC were added to the solution, then these materials were heated at 120°C with oil bath with stirrer ring reflux for 24 h, the obtained materials were then thoroughly washed with ethyl alcohol and diethyl ether solutions, respectively. Then polyamine-modified carbon was obtained and marked as AC-EDA.

Characterization of sample

N_2 adsorption–desorption isotherms were employed at 77 K to investigate the textural properties of prepared samples. Prior to adsorption, the samples were out-gassed under vacuum at 80°C for 2 h. The nitrogen adsorption amounts were converted at a relative pressure of 0.98 to the liquid nitrogen volume to obtain the total pore volume. And the S_{BET} was calculated from the Brunauer–Emmett–Teller (*BET*) equation. The micropore volumes (V_{mic}) and the mesopore volumes (V_{mes}) were calculated by t-plot method and BJH method, respectively. The pore size distribution was learned from the density functional theory (DFT). The surface functional groups of the adsorbent were detected by FTIR, 1 mg of sample and 500 mg of KBr (the ratio of KBr:sample was 500:1) were put into the agate mortar and ground well. Afterwards, they were compressed into the plate sample and then recorded between wavenumbers of 4000 and 400 cm^{-1}. The surfaces of carbons before and after Cr(III) adsorption were analyzed by XPS.

Adsorption experiments

Adsorption studies

The Cr(III) solutions were prepared from a stock chromic nitrate solution (1 g/L) and then diluted to known concentrations ranging from 0.5 to 4 mg/L, then 0.01 g of prepared carbons were placed in 250 mL Erlenmeyer flask separately and 100 mL chromic nitrate solutions with different concentrations were added into each flask. After that, the flasks were shaken in the constant temperature shaker for 24 h at 25°C, 35°C, 45°C, respectively, to attain equilibrium. The equilibrium concentration of chromic nitrate solutions was determined by A3 flame absorption spectrophotometer (the flame used acetylene-air).

Effect of pH

The HNO_3 and NaOH solutions were used to adjust the pH of the Cr(III) solutions to 2, 3, 4, 5, 6 and 8. The 0.01 g prepared carbons were put into 250 mL Erlenmeyer flask, and 100 mL concentration of 4 mg/L chromic nitrate solutions with different pH were added into it separately. Afterwards, the flasks were shaken in the constant temperature

shaker for 24 h at 25°C. Finally, the residual concentrations of chromium ion were determined by A3 flame absorption spectrophotometer.

Kinetic study

In kinetic studies, batch experiments were conducted at different periods by adding adsorbents into each 500-mL chromic nitrate solution at 25°C. Samples were collected periodically at every 5 min for the first 30 min and then at every 15 min for kinetic studies.

The adsorption amount (Qe) and removal efficiency (Re) of Cr(III) on prepared carbons can be calculated using Equations 1 and 2, respectively:

$$Q_e = V(C_o - C_e) / m \quad \text{Eq. [1]}$$

$$R_e = (C_o - C_e) / C_o \quad \text{Eq. [2]}$$

Where V is the volume of the chromic nitrate solution (L), C_e and C_0 are the solution equilibrium concentration and initial concentration (mg/L) separately, and m is the weight of the prepared carbons (g).

Result and discussion

Characteristics of the adsorbent

Analysis of surface area and pore structure characterization

The nitrogen adsorption–desorption isotherms and DFT pore size distribution for three samples (AC, AC-HNO_3 and AC-EDA) were depicted in (Fig. 1). As shown in (Fig. 1A), among the low-pressure region where P/P_0 ≤0.01, the isotherms of all samples increased rapidly, which indicated the presence of micropores (14). From the shape of the isotherms, the AC-EDA yielded isotherms intermediate between type I and type II according to IUPAC classification (15), the isotherm increased slowly then flattened out, which suggested the reaction was a molecular single layer adsorption. Furthermore, the misalignment of the adsorption and desorption curves generated a hysteresis loop in the high-pressure region where P/P_0 was in the range of 0.4-0.8, it was the occurrence of capillary condensation, showing that the modified carbon AC-EDA was developed in mesopore volumes. According to the IUPAC classification, the isotherm of AC yielded typical type IV isotherm with an obvious hysteresis loop (16), which indicated the abundance of mesopores in AC. From (Fig. 1B), it was easily observed that the pore size distribution curves

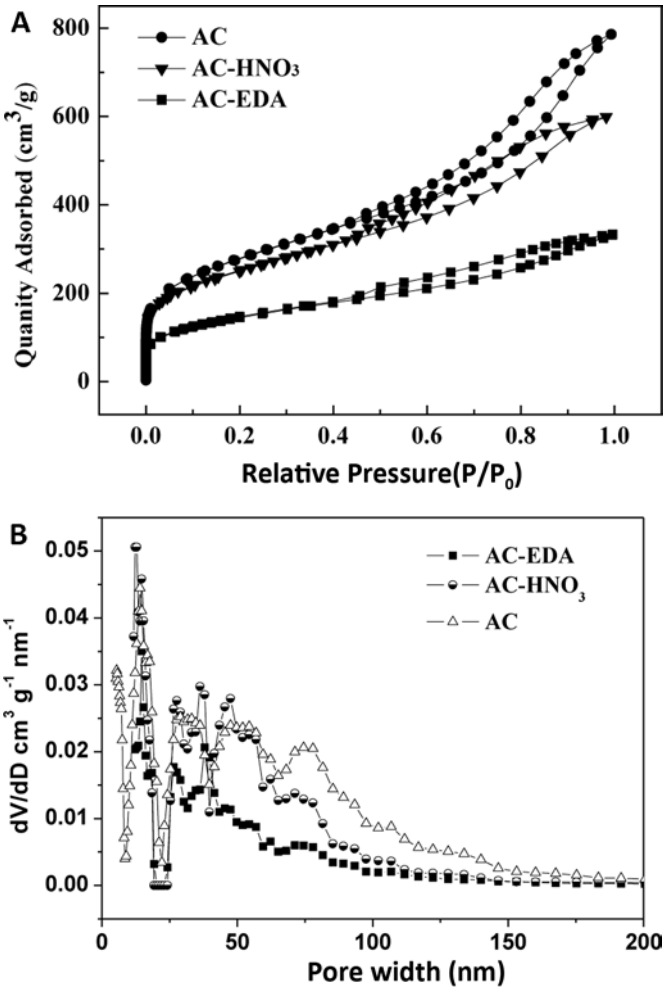

Fig. 1 - (**A**) N_2 adsorption–desorption isotherms and (**B**) pore size distribution for samples AC, AC-HNO_3 and AC-EDA.

of three samples had multiple peaks including a maximum density in the range 2-50 nm, showing that these adsorbents were dominantly mesopores. It also can be seen that the mesopore volumes decreased for AC-EDA compared with AC and AC-HNO_3; the explanation could be that after modification the surface functional groups were introduced inside the pore of AC-EDA, decreasing pore volumes.

Table I contained the total pore volumes (V_{total}), S_{BET}, mesopore volumes (V_{mes}), micropore volumes (V_{mic}) and pore size (D_p, $D_p = 4*V_{total}/S_{BET}$) results, we can see that the S_{BET} and V_{total} of carbons (AC-HNO_3, AC-EDA) were both reduced compared with pristine carbon AC, but their S_{BET} were still developed of

TABLE I - Main pore characteristics of samples

Samples	S_{BET}(m^2/g)	V_{total}(cm^3/g)	V_{mac}(cm^3/g)	V_{mic}(cm^3/g)	V_{mes}(cm^3/g)	D_p(nm)	Mesopore ratio (%)
AC	978	1.216	0.079	0.049	1.088	4.973	89.5
AC-HNO_3	890	0.926	0.149	0.049	0.728	4.162	78.6
AC-EDA	485	0.506	0.029	0.001	0.476	4.173	94.1

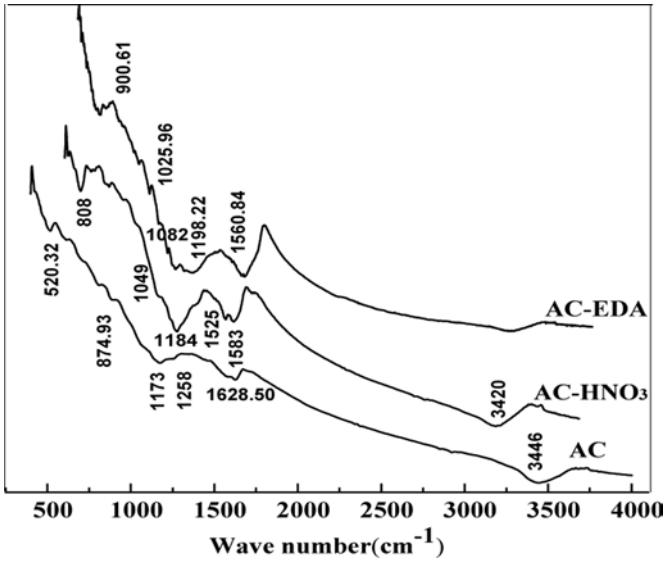

Fig. 2 - Spectra of carbon AC before and after modification.

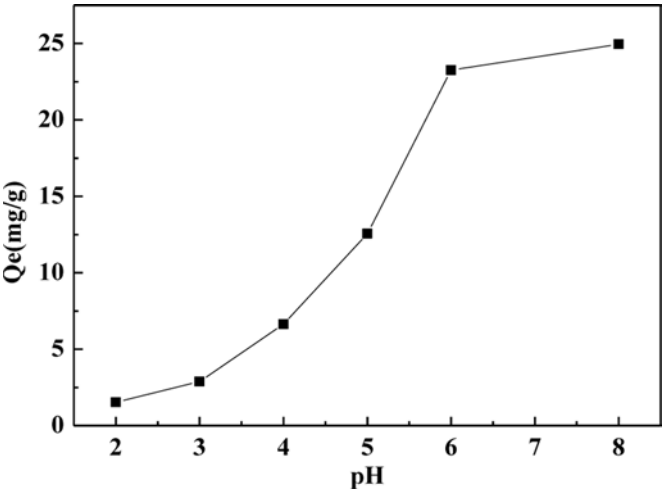

Fig. 3 - Effect of solution pH on Cr(III) adsorption onto AC-EDA. Qe = adsorption amount.

890 m^2/g and 485 m^2/g, separately. The table also showed that the percentages of mesopore volumes of AC, AC-HNO_3 and AC-EDA were 89.5%, 78.6% and 94.1%, respectively, which indicated they were all typical mesoporous carbons.

Analysis of FTIR

Figure 2 showed the FTIR spectra of prepared carbons. For AC, the band at 1173 cm^{-1} could be assigned to the stretching vibration of the ketone groups' framework that composed of C element, the band at 1600 cm^{-1} corresponded to the -COO- of carboxylic groups or the C = O of lactonic groups, the band obtained at 3446 cm^{-1} was stretching and bending mode of O-H (17), indicating some hydroxyl and carboxyl groups existed on the surface of AC. For AC-HNO_3, the band at 3446 cm^{-1} of AC was shifted to 3420 cm^{-1} and the peak narrowed, indicating the amounts of hydroxyl were decreased after oxidation; the band at 1184 cm^{-1} was assigned to the stretching vibration of C-O-C (18), the sharp band at 1583 cm^{-1} could correspond to the C = O; these bands were strong with AC-HNO_3 but invisible or weak with AC, suggesting the HNO_3 treatment efficiently increased the amounts of oxygen-containing acidic functional groups like carboxylic and lactonic groups. Compared with AC-HNO_3, the modified carbon AC-EDA was observed, new shoulders at 1198 cm^{-1} corresponded to C-N stretching, and the band at 1560.84 cm^{-1} often ascribed to the bending vibration of secondary amide (N-H) (19). The presence of surface functional groups containing nitrogen indicated the amino group was successfully introduced to the AC-EDA.

Effect of pH

The pH effect on Cr(III) adsorption onto AC-EDA was researched with the solution pH setting from 2.0 to 8.0 at 25°C. It is known that different reactions may take place in the solide-solution interface (20). As shown in (Fig. 3), we easily found that the adsorption amounts at equilibrium of Cr(III) on AC-EDA increased sharply with the increasing solution pH, but then increased slightly when the solution pH was in the range of 6.0 to 8.0. This could be due to the electrostatic interaction between the Cr(III) ions and the AC-EDA. At low pH range below pHzpc between 2.0 and 5.0, hydrogen ions competed with Cr(III) for the surface of the AC-EDA, which would prevent Cr(III) from approaching binding sites of AC-EDA caused by the electrostatic repulsive forces. Meanwhile, the electrostatic repulsion between the Cr(III) ion and the surface of protonated amino groups gradually weakened with the increasing pH (21). At pH >pHzpc, the surface of AC-EDA showed negative and developed a strong electrostatic attraction with positive Cr(III) species, thus, the Cr(III) adsorption was improved.

It was observed that further increase of the adsorption amount at higher pH (pH >6) was mainly due to the phenomenon called surface precipitation. It occurred via a surface complex reaction between the chromium ion and the carbon surface sites (Cr^{3+} and OH^- may appear in the form of $Cr(OH)_2^+$, $Cr(OH)^{2+}$ and some kind of larger hydroxy complexes) (22), which should be distinguished from the process of Cr(III) adsorption we discussed above. It was also concluded that the optimal solution pH was 6 with the maximum Cr(III) adsorption capacity reaching 24.61 mg/g. Therefore, we determined to run all Cr(III) adsorption experiments at pH = 6.0 to guarantee that the process of chromium removal would be only driven by adsorption without surface precipitation.

Effect of modification

Figure 4 depicts the Cr(III) adsorption performance of carbons with initial concentrations of chromic nitrate solution from 0.5 to 4 mg/L under 25°C, at pH 6.0. As shown in (Fig. 4A), the adsorption capacity of three carbons all increased with the increasing initial concentrations. When the initial concentration was 4.0 mg/L, the Cr(III) adsorbed amounts of pristine carbon AC were 6.36 mg/g, while the modified carbon AC-EDA on Cr(III) maximum adsorbed amounts reached 24.61 mg/g, which was 3.9 times more

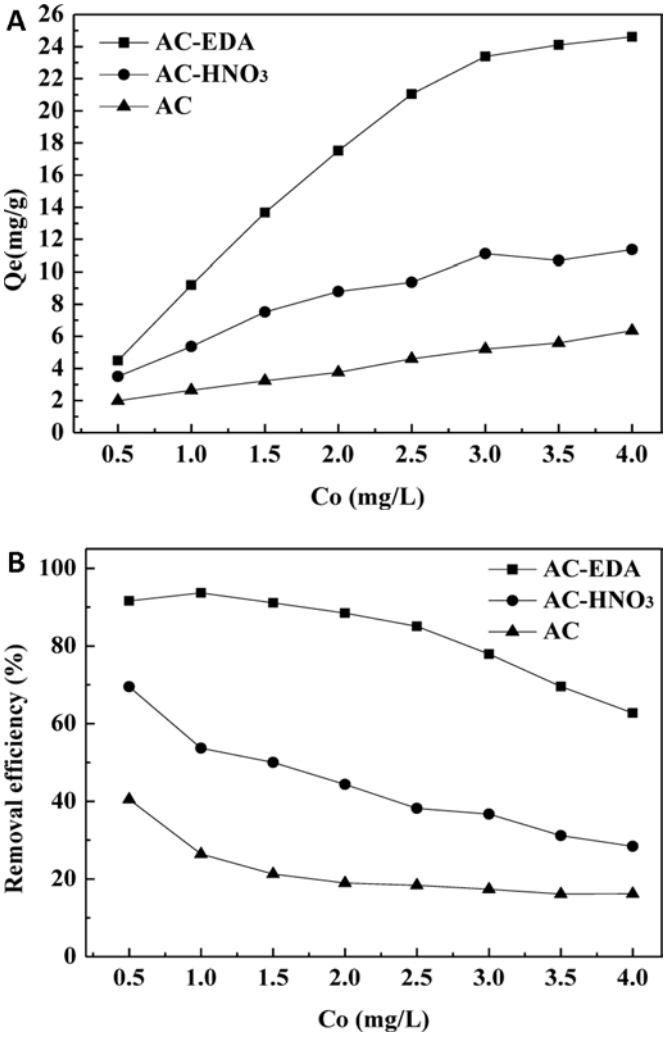

Fig. 4 - (**A**) Cr(III) adsorption capacity and (**B**) removal efficiency for different carbons AC, AC-HNO3 and AC-EDA.

than that on AC. Besides, the oxidized carbon AC-HNO_3 showed higher Cr(III) adsorption capacity compared with pristine carbon AC. As depicted in (Fig. 4B), which exhibited removal efficiency toward Cr(III) for samples, the removal efficiency of Cr(III) decreased with the increasing initial concentration for all samples. It was obvious that Cr(III) removal efficiency for AC-EDA was much higher than that for both for AC and AC-HNO_3, which reached 91.62% with the initial concentration being 0.5 mg/L, while the removal efficiencies for AC were still less than 50% throughout the initial concentrations investigated from 0.5 to 4.0 mg/L. In addition, since the removal efficiency for AC-EDA decreased but was still high as 85%, when the initial concentration increased to 2.5 mg/L, we could conclude that the optimal range of initial concentrations of chromic nitrate solution was 0.5 to 2.5 mg/L. From the above discussions, the adsorption capacity of modified carbon AC-EDA was significant prior to that for both AC and AC-HNO_3, indicating that AC-EDA with modification of EDA was beneficial to improve the adsorption capacity. Meanwhile, compared with adsorption capacities of Cr(III) on different adsorbents reported in the literature (as shown

TABLE II - The Cr(III) adsorption capacity on different adsorbents

Authors	Adsorbent	Adsorption capacity (mg/g)
Zhang (23)	Novel branched polyethyleneimine chelating resin	11.44
Han (24)	Mesoporous material MCM-48	8.25
Chen (25)	Baker's yeast	9.54
Haiwen Ma	Polyamine-modified carbon AC-EDA	24.61

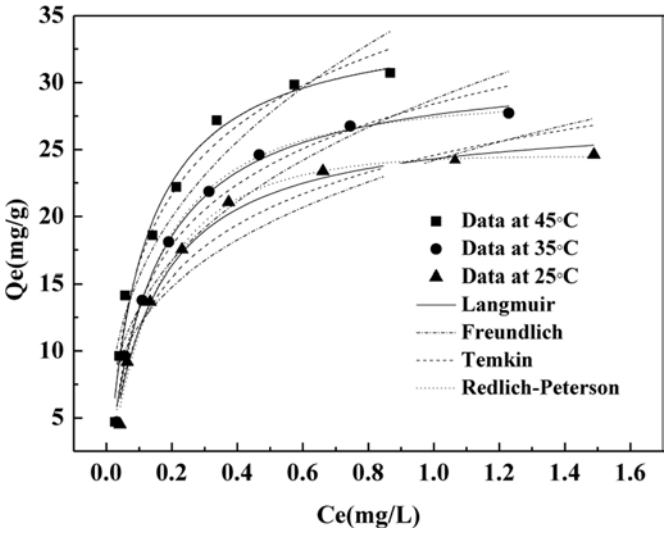

Fig. 5 - Adsorption isotherms of Cr(III) on modified carbon AC-EDA.

in Tab. II), the Cr(III) adsorption capacity for modified carbon AC-EDA [the maximum adsorbed amounts were 24.61 mg/g showed in (Fig. 4A)] was larger than those for other adsorbents in the literature (23-25), which was about three times that for the mesoporous material MCM-48. Thus, it was obvious that the polyamine-modified carbon AC-EDA developed in the present study was greatly competitive for the removal of chromium(III) ion from aqueous solutions.

Adsorption isotherms

Graphic presentations of Cr(III) adsorption on modified carbon AC-EDA at the experimental temperature of 25, 35 and 45°C, at pH 6.0 are shown in (Fig. 5). It was seen that the adsorption amounts increased with the increasing temperature, the maximum adsorbed amounts were 24.61, 27.71, 30.72 mg/g under the temperature of 25°C, 35°C and 45°C, indicating that the process of the adsorption was endothermic.

The adsorption isotherm describes how the adsorbate molecules distribute between the liquid phase and the solid phase when the adsorption process reaches an equilibrium state (26). Nonlinear models Freundlich, Langmuir, Temkin and Redlich-Peterson were applied to the adsorption iso-

TABLE III - Isotherm parameters of Cr(III) adsorption on modified carbon AC-EDA

Model	Model isotherm formula	Parameter	AC-EDA		
			25°C	35°C	45°C
Langmuir	$q_e = b\, q^{\circ} c_e / (1 + b\, c_e)$	q°(mg/g)	27.669	31.437	35.037
		b(L/mg)	7.214	7.188	9.050
		R^2	0.983	0.994	0.979
Freundlich	$q_e = K_F c_e^{1/n}$	K_F(L/mg)	24.178	28.760	35.615
		n	3.260	2.960	2.774
		R^2	0.852	0.895	0.906
Redlich-Peterson	$q_e = K_R c_e (1 + a c_e^{b})$	K_R(L/mg)	161.474	206.191	319.519
		a(L/mg)	5.660	6.525	9.112
		b	1.119	1.050	0.996
		R^2	0.989	0.995	0.974
Temkin	$q_e = b\, lnA_T + b\, lnc_e$	A_T(L/mg)	77.314	76.162	92.183
		b(L/mg)	5.649	6.555	7.424
		R^2	0.948	0.980	0.977

therm to conduct further research on the adsorption performance of Cr(III) on AC-EDA. Model equation and isothermal parameters are shown in Table III. As shown in (Fig. 5), the isotherms of Redlich-Peterson and Langmuir were approximately consistent with experimental data, but the isotherm of Freundlich was not matched so well with the data. According to the data in Table III, it can also be seen that the correlation coefficient (R^2) of Langmuir and Redlich-Peterson models were higher than that of other models. The results showed that Langmuir and Redlich-Peterson models were more suitable to fit the adsorption isotherms of Cr(III), implying that the adsorbed Cr(III) ion mainly formed monolayer coverage on the surface of modified carbon AC-EDA (27, 28).

Thermodynamic parameters include adsorption standard Gibbs free energy (*ΔG°*) entropy (*ΔS°*) and enthalpy (*ΔH°*). The *ΔG°* can be calculated by Eq. (3), the *ΔS°* and *ΔH°* were determined by plotting of lnK_D versus 1/T according to Equation 4, which were mean values at different temperatures (29).

$$\Delta G^{\circ} = -RT \ln K_D \qquad \text{Eq. [3]}$$

$$\ln K_D = \Delta S^{\circ} / R - (\Delta H^{\circ} / R) / T \qquad \text{Eq. [4]}$$

where *T* denotes the absolute temperature (K), *R* is the universal gas constant (8.314J/(mol·K)). The thermodynamic equilibrium constant K_D at different temperatures can be obtained by Equation 5 (30).

$$K_D = \alpha / \beta = (V_s Q_e) / (V_e C_e) \qquad \text{Eq. [5]}$$

Where *α* denotes the activity of adsorbed Cr(III) and *β* is the activity of Cr(III) in solution at equilibrium, V_e an V_s refer to the volume of Cr(III) in solution and the activity coefficient of adsorbed Cr(III), separately. K_D can be calculated by plotting Q_e/C_e versus Q_e and extrapolating Q_e to zero when the Cr(III) concentration in the solution decreased and approached zero (31).

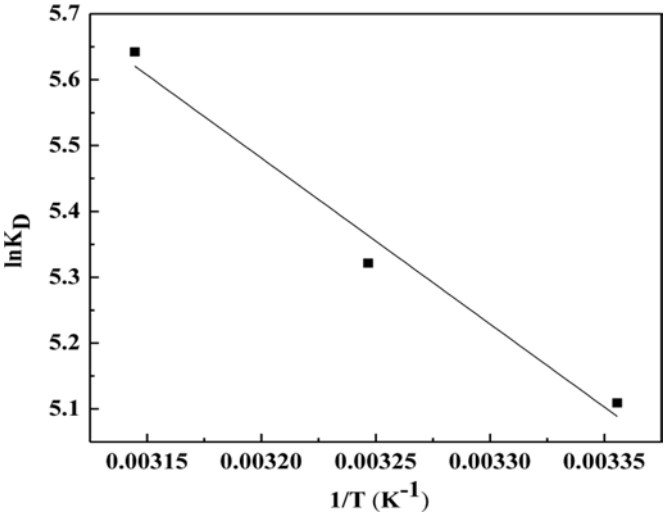

Fig. 6 - Plot of lnK_D versus 1/T for the Cr(III) adsorption on AC-EDA.

TABLE IV - Thermodynamic data for Cr(III) adsorption on AC-EDA

T(°C)	lnK_D	ΔG° (kJ/mol)	ΔH° (kJ/mol)	ΔS° J/(mol·K)
25	5.11	-12.66	20.95	112.65
35	5.32	-13.63	20.95	112.65
45	5.64	-14.92	20.95	112.65

Plot of lnK_D versus 1/T for the Cr(III) adsorption on AC-EDA is shown in (Fig. 6). Table IV shows the obtained thermodynamic parameters. It is known that these parameters could evaluate the feasibility and orientation of the physical adsorption as well as chemical adsorption (32). The change of ΔG° for the physical adsorption is generally in the range of -20 to

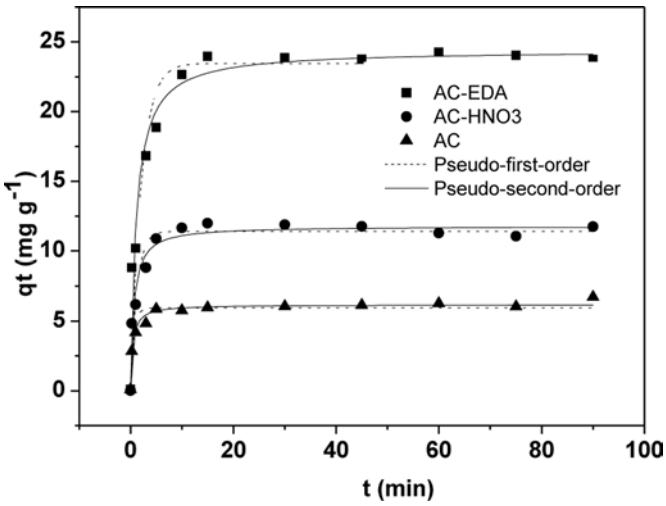

Fig. 7 - Adsorption kinetics curves of the samples.

0 kJ/mol, and that for the chemical adsorption is in the range of -400 to -80 kJ/mol (33). As shown in Table IV, the ΔG° was in the range of -14.92 to -12.66 kJ/mol, implying the adsorptive reaction was a physical process rather than chemical adsorption. However, the positive value of ΔH° showed the adsorption was endothermic. Hence the reasonable explanation of these observations was that the adsorption process was mainly driven by the electrostatic adsorption rather than van der Waals' forces (VDW) (34). The absolute value of ΔH° increased with the increasing temperature testified a higher adsorption impetus in higher temperature. Besides, the positive adsorption entropy changes (ΔS°) indicated the adsorption process was mainly driven by entropy change, it also suggested the mobility of chromium ions on AC-EDA surface became more random during the adsorption process, which could be ascribed to the replacement of water molecules on the AC-EDA surface by chromium ion (35).

Adsorption kinetics

Equilibrium time is one of the most important operational parameters for an effective wastewater treatment process. In order to investigate the kinetics of adsorption of samples, pseudo-first-order model and pseudo-second-order model (36) were used as follows (Equation 6 and Equation 7, respectively):

$$q_t = q_e - q_e e^{-k_1^t} \quad \text{Eq. [6]}$$

$$q_t = \frac{t}{1/(k_2 q_e^2) + t/q_e} \quad \text{Eq. [7]}$$

Where t is the reaction time (min), q_e and q_t (mg·g^{-1}) are the amounts of metal ion adsorbed at equilibrium and at reaction time (t), k_1 (min^{-1}) and k_2 (g·mg^{-1}min^{-1}) are the equilibrium rate constants for pseudo-first-order and pseudo-second-order models, respectively.

The effect of the time on the adsorption uptake is presented in (Fig. 7). The model parameters obtained by curve-fitting kinetic data are listed in Table V, from which it was found that the values of correlation coefficients (R^2) for the pseudo-second-order model were all higher than those for the pseudo-first-order model. Therefore, the pseudo-second-order model could be used for the prediction of the kinetics of adsorption on the adsorbents. This model is frequently used to describe kinetics of adsorption process on carbon-based adsorbents where valence forces due to the sharing or exchange of electrons between metal ions and adsorbent are involved (37).

TABLE V - Parameters of kinetic models for Cr(III) adsorption on AC, AC-HNO_3 and AC-EDA

Model	Parameters	AC	AC-HNO_3	AC-EDA
Pseudo-first-order	q_e(mg.g^{-1})	5.9549	11.401	23.471
	k_1 (min^{-1})	1.6254	0.8360	0.4911
	R^2	0.9151	0.9219	0.9229
Pseudo-second-order	q_e (mg.g^{-1})	6.1787	11.772	24.410
	k_2 (g.mg^{-1}min^{-1})	0.4081	0.1378	0.0380
	R^2	0.9699	0.9596	0.9601

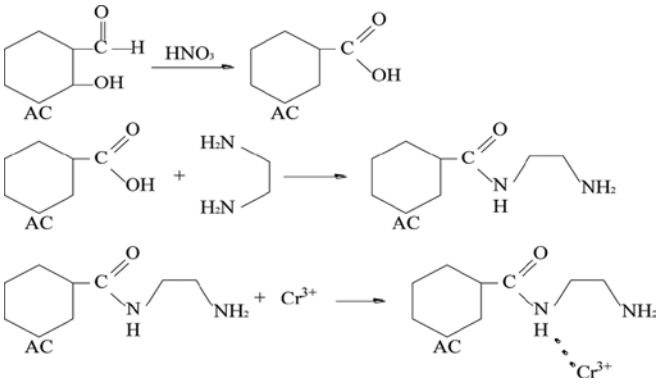

Fig. 8 - The reaction mechanism of modification and Cr(III) adsorption.

Analysis of adsorption mechanism

The bagasse-based mesoporous carbons have been successfully synthetized and modified with the treatments of nitric acid oxidization and EDA modification. From the above analysis of FTIR, it can be concluded that after HNO_3 treatment the amounts of oxygen-containing acidic functional groups like carboxyl were efficiently increased and amino groups were successfully introduced to the modified carbon after modification. The reaction mechanism of this process is shown in (Fig. 8). It was reported that the adsorption capacity of activated carbon was affected by VDW's force, electrostatic adsorption or chemical bond binding (38). As for VDW's force, the pore structure and S_{BET} were domain influence factors (39). As it can be seen from Table I, the modified carbon AC-EDA also contained macropore volumes. An explanation is that the acid oxidation broke part of the structure of micropore and mesopore, then the forming of macroporous structure enlarged pore structure, which provided an easier access for the entrance of carboxyl and amino,

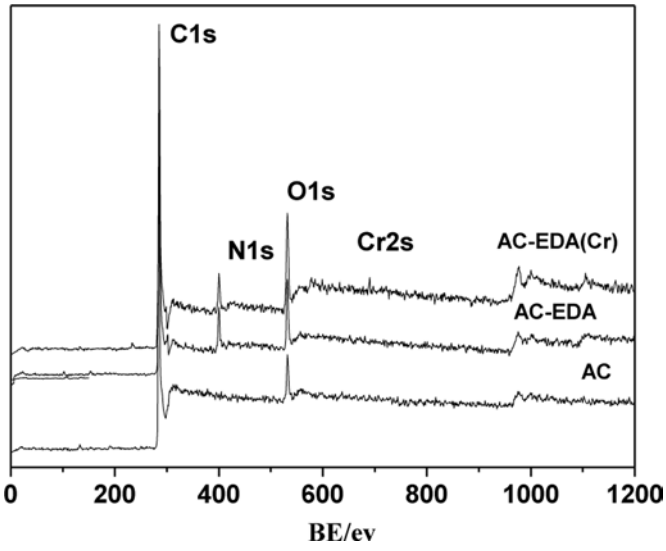

Fig. 9 - X-ray photoelectra spectroscopy (XPS) of AC, AC-EDA before and after Cr(III) adsorption.

thereby increasing carbons' adsorption amounts of Cr(III) ion. Chemical property of Cr(III) adsorption on activated carbon is rather complicated and appears to be attributable to electrostatic attraction, surface precipitation and chemical interaction between the metal ions and surface functional groups (40).

The high Cr(III) adsorption capacity of the modified carbon AC-EDA has been demonstrated from the above study. To find out the main mechanism of Cr(III) adsorption by AC-EDA, XPS was applied to study the surface chemical compositions of AC, AC-EDA before and after Cr(III) adsorption (Fig. 9). The elemental surface composition of ACs can be calculated according to the area of each element. The N element content (At.%) on AC and AC–EDA surface by XPS was 0.26 and 9.11, respectively, confirming that nitrogen functionalities were effectively embedded to the frame of AC. Compared with the AC-EDA before adsorption, the AC-EDA(Cr) after Cr(III) adsorption appeared a new peak Cr2s at the BE (binding energy) 578eV, which implied that chromium ions were adsorbed onto the surface of modified carbon successfully (41). In addition, after Cr(III) adsorption, the peak value of N1s in AC-EDA reduced from 11,866 to 6040, implying that the Cr(III) was adsorbed by combining with modified carbon AC-EDA and the nitrogen-containing function groups were the active sites for the adsorption. To sum up, the above analysis and evidence lead us to the unquestionable conclusion that the modified amino groups did contribute to the process of Cr(III) adsorption.

In fact, Pearson's theory of hard and soft acid bases could explain the efficient Cr(III) adsorption on modified carbon AC-EDA, which is also a special way of electrostatic attraction. According to the theory, the combination of soft acid and soft base, hard acid and hard base both were able to form the most stable adduct, while the combinations of soft base and hard acid or hard base and soft acid were unstable (42). After EDA modification, the AC-EDA turned into weak base and its nitrogen atom on the surface had a pair of lone electrons, while chromium ion was a kind of soft acid, which had the priority to combine with both nitrogenous groups and soft bases on carbon's surface (43). The lone pair of electrons on nitrogen atom and the empty orbit of Cr atom have formed a covalent bond, making the amino group combined with Cr(III) ions easily, so that the Cr(III) ions were absorbed onto the surface of modified carbons and finally formed the stable state, which meant the -NH_2 became the center site of Cr(III) adsorption (as shown in (Fig. 8)). Thus, it can be speculated that the amino group on AC-EDA played a vital role in the enhanced Cr(III) adsorption by electrostatic adsorption.

Conclusions

We have prepared bagasse-based mesoporous carbon, which was subsequently treated by oxidization of nitric acid and modification of EDA for the efficient Cr(III) adsorption from aqueous solutions. It has been proven that the adsorption performance of modified carbon AC-EDA was significant prior to that for both pristine and oxidized carbons, indicating the chemical modification of EDA could greatly improve the adsorption capacity of Cr(III) on activated carbon. The FTIR analysis proved that the oxidized carbon AC-HNO_3 surface was abundant in carboxyl groups and modified carbon AC-EDA was successfully grafted to amino groups. The found adsorption capacity of Cr(III) on modified carbon AC-EDA reached 24.61 mg/g at pH 6.0 under 25°C, which was much larger than those for various reported adsorbents. The adsorption was found to be significantly depended on solution pH, and the value 6.0 was selected to be the optimal solution pH for the efficient removal of Cr(III). The adsorption isotherms indicated that the adsorption of Cr(III) on modified carbon AC-EDA was an endothermic reaction. Both Langmuir and Redlich-Peterson models yielded fairly good fits to the adsorption isotherms, and it implied that the Cr(III) adsorption on AC-EDA was a homogeneous monolayer adsorption. The pseudo-second-order model could better describe the kinetic rates. The XPS energy spectrum of AC-EDA before and after Cr(III) adsorption proved that the amino group was a key factor of the efficient adsorption. Those results attested the great usefulness of obtained bagasse-based mesoporous AC-EDA toward the high efficient removal of chromium(III) ion from wastewater.

Disclosures

Financial support: The authors sincerely thank the research financial support provided by the Doctoral fund of Ministry of Education of China (20110097120021), Nanjing Agricultural University Youth Science and Technology Innovation Foundation, Nanjing Agricultural University Student Research Training Program (1530A48).
Conflict of interest: None of the authors has financial interest related to this study to disclose.

References

1. Shankar AK, Venkateswarlu B. Chromium: environmental pollution, health effects and mode of action A2. In: Nriagu JO, ed. Encyclopedia of environmental health. Elsevier, Burlington, 2011;650-659.
2. Li L, Liu F, Duan H, et al. The preparation of novel adsorbent materials with efficient adsorption performance for both chromium

and methylene blue. Colloids Surf B Biointerfaces. 2016;141: 253-259.
3. Hosseini S, Masoudi Soltani S, Jahangirian H, Eghbali Babadi F, Choong TSY, Khodapanah N. Fabrication and characterization porous carbon rod-shaped from almond natural fibers for environmental applications. Journal of Environmental Chemical Engineering. 2015;3(4):2273-2280.
4. Marco-Lozar JP, Linares-Solano A, Cazorla-Amorós D. Effect of the porous texture and surface chemistry of activated carbons on the adsorption of a germanium complex from dilute aqueous solutions. Carbon. 2011;49(10):3325-3331.
5. Pant D, Singh P. Chemical modification of waste glass from cathode ray tubes (CRTs) as low cost adsorbent. Journal of Environmental Chemical Engineering. 2013;1(3):226-232.
6. Lorenc-Grabowska E, Diez MA, Gryglewicz G. Influence of pore size distribution on the adsorption of phenol on PET-based activated carbons. J Colloid Interface Sci. 2016;469:205-212.
7. Wang Z, Shi M, Li J, Zheng Z. Influence of moderate pre-oxidation treatment on the physical, chemical and phosphate adsorption properties of iron-containing activated carbon. J Environ Sci (China). 2014;26(3):519-528.
8. Liu F, Guo Z, Ling H, Huang Z, Tang D. Effect of pore structure on the adsorption of aqueous dyes to ordered mesoporous carbons. Microporous and Mesoporous Mater. 2016;227:104-111.
9. Liu J, Li Y, Li Y, Sang S, Li S. Effects of pore structure on thermal conductivity and strength of alumina porous ceramics using carbon black as pore-forming agent. Ceram Int. 2016;42(7):8221-8228.
10. Lee H-M, Kim H-G, Kang S-J, Park S-J, An K-H, Kim B-J. Effects of pore structures on electrochemical behaviors of polyacrylonitrile (PAN)-based activated carbon nanofibers. J Ind Eng Chem. 2015;21:736-740.
11. Liu J, Cheney MA, Wu F, Li M. Effects of chemical functional groups on elemental mercury adsorption on carbonaceous surfaces. J Hazard Mater. 2011;186(1):108-113.
12. Pradhan S, Singh S, Rai LC. Characterization of various functional groups present in the capsule of Microcystis and study of their role in biosorption of Fe, Ni and Cr. Bioresour Technol. 2007;98(3):595-601.
13. Zhiqiang Zhu Kunquan Li. Preparation and its influence factors of mesoporous activated carbon from bagasse with phosphoric acid activation at low temperature. Chinese Journal of Environmental Engineering. 2015;6:2667-2673.
14. Ling X, Li J, Zhu W, et al. Synthesis of nanoscale zero-valent iron/ordered mesoporous carbon for adsorption and synergistic reduction of nitrobenzene. Chemosphere. 2012;87(6):655-660.
15. Llorens J, Pera-Titus M. Influence of surface heterogeneity on hydrogen adsorption on activated carbons. Colloids Surf A Physicochem Eng Asp. 2009;350(1-3):63-72.
16. Ramirez A, Sierra L, Mesa M, Restrepo J. Simulation of nitrogen adsorption desorption isotherms. Hysteresis as an effect of pore connectivity. Chem Eng Sci. 2005;60:4702-4708.
17. Kim DW, Cha DK, Wang J, Huang CP. Heavy metal removal by activated sludge: influence of Nocardia amarae. Chemosphere. 2002;46(1):137-142.
18. Canaria CA, Lees IN, Wun AW, Miskelly GM, Sailor MJ. Characterization of the carbon-silicon stretch in methylated porous silicon - observation of an anomalous isotope shift in the FTIR spectrum. Inorg Chem Commun. 2002;5(8):560-564.
19. Tang L, Yang G-D, Zeng G-M, et al. Synergistic effect of iron doped ordered mesoporous carbon on adsorption-coupled reduction of hexavalent chromium and the relative mechanism study. Chem Eng J. 2014;239:114-122.
20. Huang S-H, Chen D-H. Rapid removal of heavy metal cations and anions from aqueous solutions by an amino-functionalized magnetic nano-adsorbent. J Hazard Mater. 2009;163(1):174-179.
21. Barczak M, Michalak-Zwierz K, Gdula K, et al. Ordered mesoporous carbons as effective sorbents for removal of heavy metal ions. Microporous Mesoporous Materials. 2015;211: 162-173.
22. Wang T, Liu W, Xiong L, Xu N, Ni J. Influence of pH, ionic strength and humic acid on competitive adsorption of Pb(II), Cd(II) and Cr(III) onto titanate nanotubes, Chemical Engineering Journal. 2013;s215-216:366-374.
23. Zhang C, Liu D, Wang T. Preparation and adsorption studies of novel branched poly(ethyleneimine) chelating resins. Ion Exchange and Adsorption. 2006;84-88.
24. Han Y. Adsorption of heavy metal ions on functionalized mesoporous materials. Zhejiang Normal University, 2012. http://kns.cnki.net.
25. Chen Y. Study on the baker's yeast and its immobilization on adsorbing and removing chromium ion. SiChuan Agriculture University, 2009. http://kns.cnki.net.
26. Kumari M, Pittman CU Jr, Mohan D. Heavy metals (chromium (VI) and lead (II)) removal from water using mesoporous magnetite (Fe_3O_4) nanospheres. J Colloid Interface Sci. 2015;442:120-132.
27. Abu-Zurayk RA, Al Bakain RZ, Hamadneh I, Al-Dujaili AH. Adsorption of Pb(II), Cr(III) and Cr(VI) from aqueous solution by surfactant-modified diatomaceous earth: Equilibrium, kinetic and thermodynamic modeling studies. Int J Miner Process. 2015;140:79-87.
28. Fouladi Tajar A, Kaghazchi T, Soleimani M. Adsorption of cadmium from aqueous solutions on sulfurized activated carbon prepared from nut shells. J Hazard Mater. 2009;165(1-3): 1159-1164.
29. Meena AK, Mishra GK, Rai PK, Rajagopal C, Nagar PN. Removal of heavy metal ions from aqueous solutions using carbon aerogel as an adsorbent. J Hazard Mater. 2005;122(1-2): 161-170.
30. Li Y-H, Di Z, Ding J, Wu D, Luan Z, Zhu Y. Adsorption thermodynamic, kinetic and desorption studies of Pb2+ on carbon nanotubes. Water Res. 2005;39(4):605-609.
31. Niwas R, Gupta U, Khan AA, Varshney KG. The adsorption of phosphamidon on the surface of styrene supported zirconium (IV) tungstophosphate: a thermodynamic study. Colloids Surf A Physicochem Eng Asp. 2000;164(2-3):115-119.
32. Lai C, Guo X, Xiong Z, et al. A comprehensive investigation on adsorption of Ca (II), Cr (III) and Mg (II) ions by 3D porous nickel films. J Colloid Interface Sci. 2016;463:154-163.
33. Zheng K, Pan B, Zhang Q, et al. Enhanced adsorption of p-nitroaniline from water by a carboxylated polymeric adsorbent. Separ Purif Tech. 2007;57(2):250-256.
34. Plazinski W, Rudzinski W, Plazinska A. Theoretical models of sorption kinetics including a surface reaction mechanism: a review. Adv Colloid Interface Sci. 2009;152(1-2):2-13.
35. Scheufele FB, Módenes AN, Borba CE, et al. Monolayer–multilayer adsorption phenomenological model: Kinetics, equilibrium and thermodynamics. Chem Eng J. 2016;284: 1328-1341.
36. Ma X, Cui W, Yang L, Yang Y, Chen H, Wang K. Efficient biosorption of lead(II) and cadmium(II) ions from aqueous solutions by functionalized cell with intracellular CaCO3 mineral scaffolds. Bioresour Technol. 2015;185:70-78.
37. Alikhani M, Moghbeli MR. Ion-exchange polyHIPE type membrane for removing nitrate ions: Preparation, characterization, kinetics and adsorption studies. Chem Eng J. 2014;239: 93-104.
38. Machida M, Fotoohi B, Amamo Y, Ohba T, Kanoh H, Mercier L. Cadmium(II) adsorption using functional mesoporous silica and activated carbon. J Hazard Mater. 2012;221-222: 220-227.
39. Dobrowolski R. Application of activated carbons for the enrichment of toxic metals and their determination by atomic

spectroscopy. In:Dobrowski R, ed. Studies in surface science and catalysis. Elsevier, 1999:777-805.
40. Wang J, Zheng S, Shao Y, Liu J, Xu Z, Zhu D. Amino-functionalized Fe(3)O(4)@SiO(2) core-shell magnetic nanomaterial as a novel adsorbent for aqueous heavy metals removal. J Colloid Interface Sci. 2010;349(1):293-299.
41. Liu J, Li Y, Li K. Optimization of preparation of microporous activated carbon with high surface area from Spartina alterniflora and its p-nitroaniline adsorption characteristics. Journal of Environmental Chemical Engineering. 2013;1(3): 389-397.
42. Yu J, Tong M, Sun X, Li B. A simple method to prepare poly(amic acid)-modified biomass for enhancement of lead and cadmium adsorption. Biochem Eng J. 2007;33(2):126-133.
43. Yang G, Tang L, Cai Y, et al. Effective removal of Cr(vi) through adsorption and reduction by magnetic mesoporous carbon incorporated with polyaniline. RSC Advances. 2014;4(102): 58362-58371.